Fracture Characterization of Low-Density Polyethylenes by the Essential Work of Fracture: Changes Induced by Thermal Treatments and Testing Temperature

J. J. CASELLAS,[1] P. M. FRONTINI,[1,2] J. M. CARELLA[1,2]

[1] Instituto de Investigaciones en Ciencia y Tecnología de Materiales (INTEMA) (CONICET-UNMdP), J.B. Justo 4302, (7600) Mar del Plata, Republic of Argentina

[2] Departamento de Materiales, Facultad de Ingeniería, Universidad Nacional de Mar del Plata, J.B. Justo 4302, (7600) Mar del Plata, Republic of Argentina

Received 12 November 1998; accepted 14 January 1998

ABSTRACT: The tensile deformation and fracture behavior of commercially available low-density polyethylene (LDPE) films, having different molecular characteristics, was studied. Submitting samples to specific thermal histories controlled the morphological structure of these semicrystalline polymers. Phase-structure analysis of the resulting materials was performed by DMA and DSC analyses. The plane-stress essential work of fracture methodology was chosen because the materials used had failed after complete necking of the remaining ligament. Significant differences in behavior, induced by thermal treatments, were found for the tensile yield stress and the specific nonessential work of fracture, but not in the specific essential work of fracture. The results show that the mechanical properties and fracture behavior depend not only on the crystallinity levels and molecular weight characteristics of the samples, but also upon the degree of structural continuity. The β-relaxation process, associated with the crystal-amorphous interphase, strongly influences the fracture behavior at testing temperatures chosen below the β-relaxation temperature. © 1999 John Wiley & Sons, Inc. J Appl Polym Sci 74: 781–796, 1999

Key words: low-density polyethylene; essential work of fracture; thermal treatment

INTRODUCTION

The theory of linear elastic fracture mechanics (LEFM) deals with fractures occurring at nominal stresses that are well below the uniaxial yield stress of the material. For ductile materials, this requirement cannot be achieved, because a large plastic zone is formed prior to crack initiation, violating the limits of small-scale yielding which ensures the validity of the LEFM. Usually, the *J*-integral approach proposed by Rice[1] has been used to characterize the fracture behavior for ductile materials, as an alternative to LEFM. To characterize fracture by its critical parameter J_C, a specimen must also meet size requirements, which guarantee the *J*-integral to be obtained under plane-strain conditions; these requirements are impossible to meet for thin films.

Recently, another approach was used to characterize the fracture mechanics of some ductile polymers[2,3] which cannot reach plane-strain conditions even under *J*-controlled conditions: the essential work of fracture method.[4,5] In this method, the total work of fracture (W_f) is considered to be made of two components: one considered to be nonessential (W_p), associated with plas-

Correspondence to: J. M. Carella.

Journal of Applied Polymer Science, Vol. 74, 781–796 (1999)
 CCC 0021-8995/99/040781-16

tic work in the outer plastic zone, and the essential work of fracture (W_e), associated with fracture work in the inner process zone and the initiation of instability and regarded as a material property characterizing fracture under plane-stress conditions. Physically, W_e is the work required to create two new fracture surfaces. In the fracture of ductile polymers, W_e is used to form and break the necked zone ahead of the crack tip.

Conventional (branched, high-pressure) low-density polyethylene (LDPE) and linear low-density polyethylene (LLDPE) are mainly used in the field of packaging films, where puncture and tear resistance play a very significant role. The influence of structural and morphological factors on their traditional mechanical properties[6] has already been determined for model polymers representing a wide range of molecular weight, molecular weight distributions, chemical compositions, and molecular structure and statistics; however, their fracture behavior has not been studied deeply, probably because their extraordinarily high toughness makes meeting of the plane-strain conditions on these materials[7,8] at room temperature and relatively low strain rates very difficult. Moreover, empirical, pseudoquantitative, or nonintrinsic methods such as the Elmendorf tearing test[9] have been commonly adopted by industry to provide some evaluation of their fracture toughness and stable crack propagation mode. These tests do not provide engineering designing parameters and do not clearly distinguish between initiation and propagation stages.

This article was focused on the study of the fracture behavior of commercially available LDPE and LLDPE. It reports the results of an experimental evaluation of the essential work of fracture and tensile deformation of commercially available LDPE. The results have been interpreted in terms of different supermolecular structures generated from the differences in molecular architecture and branching statistics of each polymer and also from the thermal treatments the material had undergone before testing. In addition, the influence of the testing temperature was also established upon the linear low-density polymer.

METHODOLOGY

Broberg[10] suggested that the total work of fracture, W_f, may be partitioned into two parts: the work into the end region in the vicinity of the crack tip which initiates the crack, W_e—also called the essential work of fracture—and the work into the outer region which is responsible for plastic deformation, W_p, also called the nonessential work of fracture; that is:

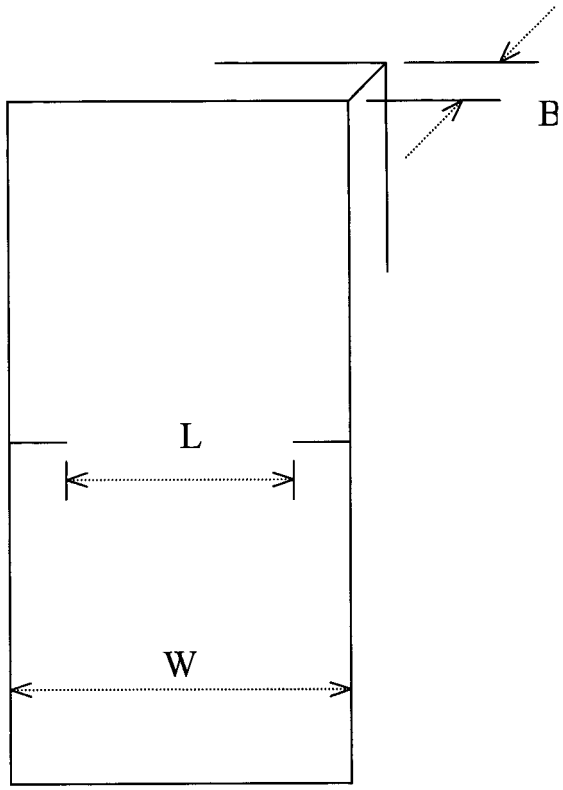

Figure 1 Double-edge notched tension (DENT) specimens used for fracture experiments.

$$W_f = W_e + W_p \tag{1}$$

The essential work of fracture, W_e, is proportional to the ligament length, L (see Fig. 1). The nonessential work of fracture, W_p, is proportional to L^2; then

$$W_f = LBw_e + L^2B\beta w_p \tag{2}$$

where B is the specimen thickness; L, the ligament length; w_e, the specific essential work of fracture—defined as the essential work in the specimen with unit thickness and unit ligament length—and w_p, the specific nonessential work of fracture. β is a shape factor for the outer plastic zone and its value depends on the specimen and crack geometry. Therefore, the total specific fracture work, w_f, may be defined as

$$w_f = w_e + L\beta w_p \quad (3)$$

The specific work of fracture, w_f, is a linear function of ligament length, L. The specific essential fracture work, w_e, is a material constant for a given sheet thickness and may be a useful material constant for characterizing the fracture toughness of ductile materials. w_p is the nonessential work of fracture dissipated per unit volume of the material, and it is not a material property. w_p is expected to increase with ductility of the material and to vanish for brittleness.[11]

EXPERIMENTAL

Materials and Sample Preparation

Two types of LDPE were used: linear PE 6220/1 (LLDPE), MI 2 g/10 min, nominal density 0.920; and PE 2120 /1 (LDPE), MI 2 g/10 min, nominal density 0.920. Both materials were kindly supplied by IPAKO S.A. (Bahia Blanca, Republica Argentina) in the form of stabilized pellets. A binary blend was also prepared by melt-mixing in a Brabender-like apparatus at 150°C and 50 rpm for 10 min. The composition of the binary system LLDPE/LDPE was (wt/wt) 80/20 (blend). This composition was chosen because its reported Elmendorf tear resistance is higher than are the values for pure PE 6220 and PE 2120.[12]

The blend is commercially available and widely used because of the excellent properties of films made from it. Pellets were first vacuum-molded at 145°C, as plates of 0.65-mm thickness, and quickly cooled to room temperature with running water. Afterward, the plates were placed between two flat metal sheets and heated in an oven at 145°C for 10 min under a very slight applied pressure to allow complete melting, using spacers between the metal sheets to obtain films of 0.27-mm nominal thickness. Subsequently, two patterns of thermal treatments were applied to the films.

Annealed samples used in this study are identified as (*A*), and quenched samples are identified as (*Q*). Annealing (*A*) consisted of quickly lowering the oven temperature to 117°C, keeping the films at 117°C for 24 h, and then letting them to cool to room temperature in air. The annealing temperature was chosen right above the melting temperature range for PE 2120 and below the temperature range where the linear PE 6220 fraction with fewer short-chain branching melts. In this way, some segregation was expected to occur in the annealed blends. A more detailed explanation of reasons for choosing this annealing temperature is included in the Discussion section. Quenching (*Q*) consisted of quenching the remelted films by plunging them in a methanol–dry ice slush.

Dynamic Mechanical Analysis

Measurements were carried out on vacuum-molded specimens using a Perkin–Elmer DMA-7e at a fixed frequency of 1 Hz and operating in a three-point bending mode. The samples used were molded to achieve a 0.7-mm nominal thickness and a 10-mm span was used throughout. Temperature calibrations were performed with indium and zinc standards. The temperature range investigated was −50 to 80°C, and the temperature was scanned at a rate of 10°C/min. Simple calculations show that for PE samples 1 mm thick, heated at a rate of 10°C/min, the maximum expected temperature differences between the sample outer layers and the center are smaller than 2°C. Also, preliminary tests were run at 2 and 5°C/min, and no significant differences were found with runs performed at 10°C/min. The samples used for the DMA measurements were conditioned with a thermal history as close as possible to that applied to the samples used for the mechanical (nominal stress-elongation and fracture) measurements, as detailed below. DMA measurements were performed after a 2-h storage at the temperature used for mechanical testing; after this storage, the DMA oven temperature was lowered to about 30°C below the storage temperature, and scans were started at that point to preserve the semicrystalline structure developed at the storage temperature

Thermal Analysis

Differential scanning calorimetry (DSC) measurements were carried out with a DuPont 990-DSC and a Shimadzu DSC-50, at a scanning rate of 10°C/min. The DuPont 990-DSC is older equipment, but it allows samples to be conditioned—in a wide temperature range—for 2 h before scanning. This feature was used to give to the samples used for DSC measurements a thermal history as close as possible to that applied to the samples used for mechanical (nominal stress-elongation and fracture) measurements, as detailed below. Thus, endotherms for all samples tested at tem-

peratures different from room temperature were obtained after a 2-h storage at the temperature used for mechanical testing; after this storage, the DSC temperature was lowered to about 30°C below the storage temperature, and scans were started at that point to preserve the semicrystalline structure developed at the storage temperature. Standard calibrations were performed with indium and tin. The degree of crystallinity was calculated from the measured melting enthalpy, taking the melting enthalpy for pure PE crystal as 69 cal/g.[13] For melting-enthalpy calculations, a straight baseline was drawn, always starting from 30°C and ending at the tangent curve after the melting temperature range.

Nominal Stress-Elongation Measurements

Dumbbell-shaped specimens were cut out of from the molded sheets with a die and stretched at a crosshead speed of 10 mm/min in a Shimadzu Universal S-500-C testing machine equipped with a thermostatic chamber that allows testing the samples from −35 to 200°C. As detailed above for DSC measurements, samples tested at temperatures different from room temperature were stored for 2 h in the thermostatic chamber—at the testing temperature—before running the tests.

The yield stress was determined—in the way conventionally accepted for polymers[14]—as the point where the force-elongation curve shows a local maximum. The gauge length of the specimens was 30 mm and the width was 6 mm. The draw ratio, λ_B, was determined at break as the ratio between initial and final length of the sample. The values reported for the draw ratio at break are averages from five specimens. Grip separation was taken as the extension. Samples tested at −25°C inside the thermostatic chamber can be only extended to over 500%, because at this point, the machine extension limit is reached.

Fracture Experiments

Tests were performed on double-edge notched tension (DENT) specimens, whose overall dimensions were 20 mm (W) × 60 mm × 0.27 mm (B; see Fig. 1). Ligament lengths (L) varied from 1 to 8 mm. Symmetrical double-edge notches were first cut by sliding a cutter and then carefully sharpened by pressing a new razor blade to a depth of 1 mm. Specimens were fractured in a Shimadzu testing machine, at a constant crosshead rate of 10 mm/min, and at temperatures of −25, 20, and 30°C. As detailed above for DSC and the stress-elongation measurements, samples tested at temperatures different from room temperature were stored for 2 h in the thermostatic chamber—at the testing temperature—before running the test.

For the essential work of fracture method to be successful, the ligament should yield prior to tear initiation at the notch tip. To avoid the plane strain–plane stress transition region,[15] the ligament must be greater than three times the specimen thickness, and to prevent edge effects, it is recommended that the ligament length be kept smaller than one-third of the sample width, particularly when double-edge-notched tension specimens are used. The following size criterion[16]

$$3B \leq L \leq \min(W/3,\ 2r_p) \tag{4}$$

where W is the sample width, and r_p, the plastic radius, was always satisfied.

Crack-opening displacement (COD) was also estimated by plotting the ultimate elongation, δ, against the ligament length. As proposed by Hashemi and O′Brien,[17] who stated that, assuming a parabolic shape for the load-displacement diagrams and the validity of Hill plasticity theory,[18] the final (break) elongation follows a linear form:

$$\delta = \frac{\text{constant}}{\sigma_y}\,(w_e + L\beta w_p) \tag{5}$$

Elongation at break for ligament length $L = 0$ represents the COD of the advancing crack tip.

RESULTS AND DISCUSSION

Thermal Treatments

In analyzing the yielding processes, the key problem is to assess the load-bearing contributions from the major structural regions. These are the ordered core crystalline region, the crystal-amorphous interphase region, and the isotropic amorphous region, where the chain units are in disordered conformation. To obtain information about the phase structure, we used DSC and DMA analyses, which provide information on the relative fractions of each one of the phases present, the relaxation processes present in the used temper-

ature range, and also on the effect of the thermal treatments.

To properly focus the following discussion, it is convenient to remark on some differences in the molecular structures of high-pressure LDPE (PE 2120/1) and LLDPE made in the gas-phase Unipol process (PE 6220/1). LLDPE is made by copolymerization and has a linear molecular backbone with short branches formed by the comonomer (usually butene or hexene). There is a broad intermolecular short-chain branching distribution associated with the copolymerization system used, which produces from highly branched to almost linear (unbranched) polymer. The cooling of the homogeneous melt of such a broad copolymer composition may result in complex morphological solid systems: a highly interconnected distribution of lamellar crystals of varying thickness—interconnected by molecules traversing more than one lamellae—can be obtained; also, during the cooling and crystallization process, there is a kinetically controlled liquid–liquid phase separation (segregation) of the most highly branched polymer fractions from the rest. Annealing and slow crystallization favor the liquid–liquid phase separation of the most highly branched polymer fractions.[19] This phase separation gives origin to a better mechanical interconnection of the crystalline lamellae.

High-pressure LDPE is made by homopolymerization and presents a much more uniform branching distribution. It is difficult to produce much segregation by crystallization in this type of polymer, but semicrystalline morphology is affected by differences in cooling rates, as can be determined from mechanical measurements. It is expected that blends of LDPE and LLDPE will show different behavior, depending on the blends' compositions.

Typical DSC endotherms are shown in Figure 2(a,b), while crystallinity and melting temperatures are specified in Tables I and II. Thermal treatments have small influence on the DSC-measured crystallinity values, as shown in Table I.

While a significant change was not found in the crystallinity after thermal treatments, changes in the forms of the melting endotherms and melting peaks are evident. Endotherms for samples rapidly crystallized from the melt (*Q*) displayed single peaks, suggesting some degree of cocrystallization between LDPE and LLDPE. Two well-defined endothermic peaks were displayed in the melting endotherms corresponding to LLDPE (*A*) and the blend (*A*), as annealing promotes partial

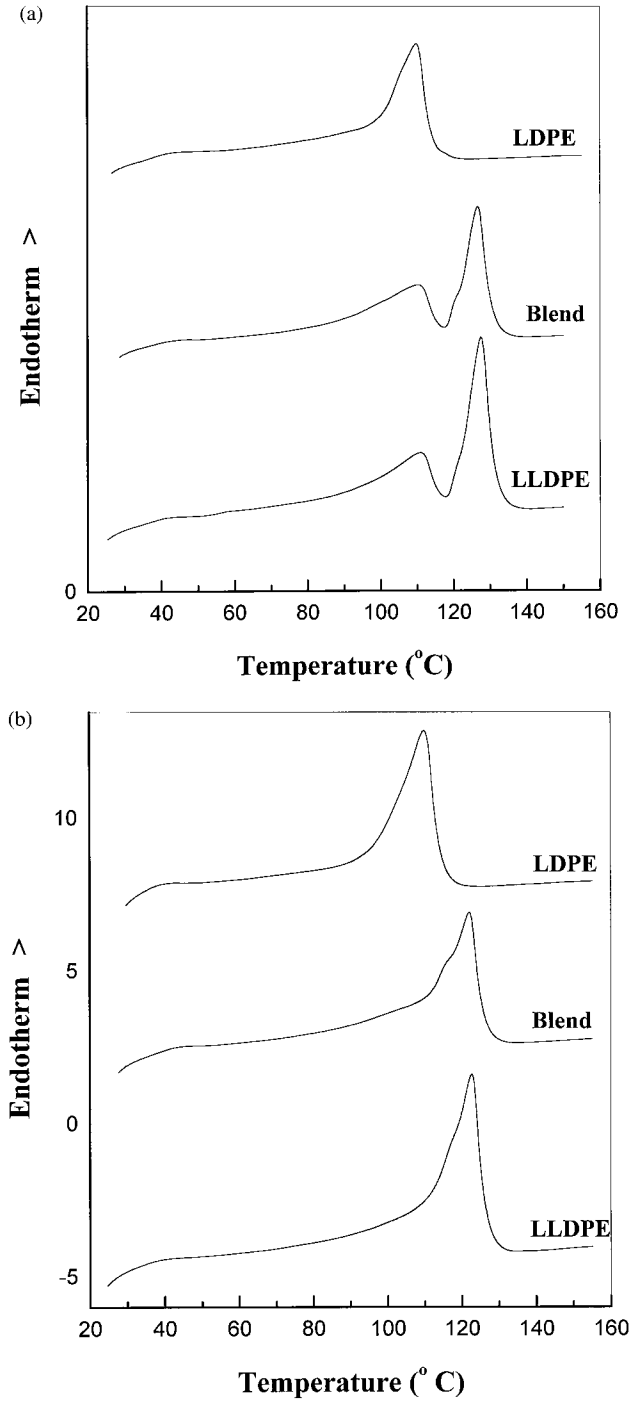

Figure 2 (a) DSC endotherms of annealed materials; (b) DSC endotherms of quenched materials.

segregation of the fractions with different degrees of branching.[20,21] The higher-temperature peaks correspond to melting of the crystals of LLDPE fractions with a lower degree of branching. The lower-temperature peaks correspond to the melting of crystals formed during air cooling from the

Table I Crystallinity and Peak Temperature Values for Samples Tested at 20°C

Sample	Thermal	X_c	T_{peak}
LLDPE	Annealing	42	110.5 127.5
LDPE	Annealing	35	110 —
Blend	Annealing	40	110 127
LLDPE	Quenching	40	123 —
LDPE	Quenching	34	110 —
Blend	Quenching	38	122 —

annealing temperature (117°C) and can be safely assigned to cocrystallized LDPE and highly branched fractions of LLDPE. It may be noticed the shift of the melting peaks for the LLDPE (*A*) and blend (*A*) samples, from 123°C corresponding to (*Q*) samples to 127°C, which is a clear indication for much thicker lamellae present in the segregated LLDPE fractions with a lower degree of branching. LDPE crystallinity was not affected by the annealing treatment since it was done at a temperature over its melting peak. Table II exhibits the values of crystallinity developed further, when samples were held for 2 h—before mechanical testing—in the thermostatic chamber, at testing temperatures.

The temperature range used in the DMA measurements includes two major relaxation processes: the β-relaxation process, associated with the crystal-amorphous interphase, in the range of -50 to -10°C,[6] and the α-relaxation process, which corresponds to crystalline core relaxations and is closely related to lamellar thicknesses, roughly in the range of 0–140°C.[6]

As can be seen from the DMA measurements [see Fig. 3(a–d)], the mechanical response from all (*A*)-type samples show higher values for the storage modulus than do the corresponding (*Q*)-type samples, in the whole measuring temperature range, indicating a different mechanical interconnection of the crystalline lamellae

The β-relaxation process can be clearly observed in the loss modulus curves for the (*Q*)-type samples, as a smooth peak in the -40 to -10°C zone. For (*A*)-type samples, the corresponding

Table II Crystallinity and Peak Temperature Values for Samples Tested at −25, 20, and 30°C

Sample	Thermal Treatment	X_c	T_{peak}	
LLDPE	Annealing plus 2 h at −25°C	45	112.5	127.5
	Quenching plus 2 h at −25°C	42	124	—
	Annealing plus 2 h at 30°C before	43	112	127
	Quenching plus 2 h at 30°C before	41	123	—
	Annealing—tested at 20°C	42	110.5	127.5
	Quenching—tested at 20°C	40	123	—
LDPE	Annealing—tested at 20°C	35	110	—
	Quenching—tested at 20°C	34	110	—
Blend	Annealing—tested at 20°C	40	110	127
	Quenching—tested at 20°C	38	122	—

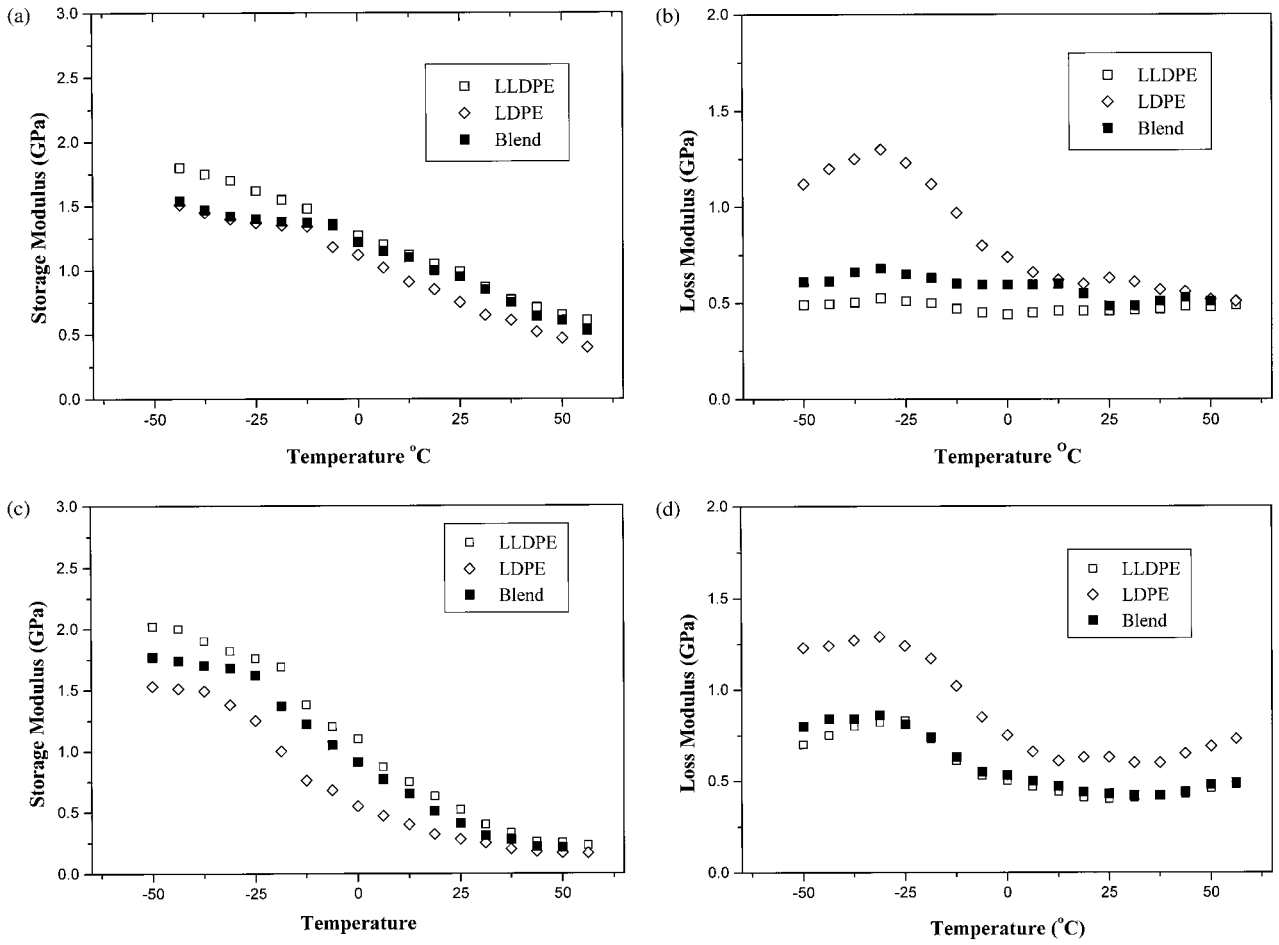

Figure 3 DMA data: (a) storage modulus for annealed samples; (b) loss modulus for annealed samples; (c) storage modulus for quenched samples; (d) loss modulus for quenched samples.

peak is not as clearly defined, and the smaller peak area also seems to be associated with a smaller fraction of the crystal-amorphous interphase. This fact corresponds to the more continuous crystalline lamellae mechanical interconnections present in the (*A*)-type samples, which may justify the much higher storage modulus values measured for these samples which show only a minor increase in crystallinity. This type of behavior has been shown to depend on the intercrystalline mechanical interconnection, which we also call semicrystalline structure continuity.[22] The elastic modulus for samples with supermolecular structures where the semicrystalline structure is more continuous has a smaller dependence on the temperature over the β-relaxation-process temperature range.[22] Also, the storage modulus curves measured for all (*A*)-type samples show a smaller effect of the β-relaxation process, which produces a shallower slope in the storage modulus curves in the -40 to -10°C zone.

The LLDPE fraction with a lower melting point is slightly segregated, as seen in the DSC measurements [Fig. 2(a)], keeping most of the interphase associated to its semicrystalline structure.[6] The LLDPE fraction with the higher melting point crystallizes in a much more ordered manner, with a minimum of interphase associated with it; this LLDPE fraction structure (with a higher crystallinity) also supports most of the applied stress,[21] and, therefore, the mechanical response becomes much less sensitive to the β-relaxation process. Quenched samples show a more homogeneous structure, characterized by a better-defined β-relaxation process as shown in the corresponding loss modulus curves.

The segregated structure with the higher crystallinity and higher melting point also produces a

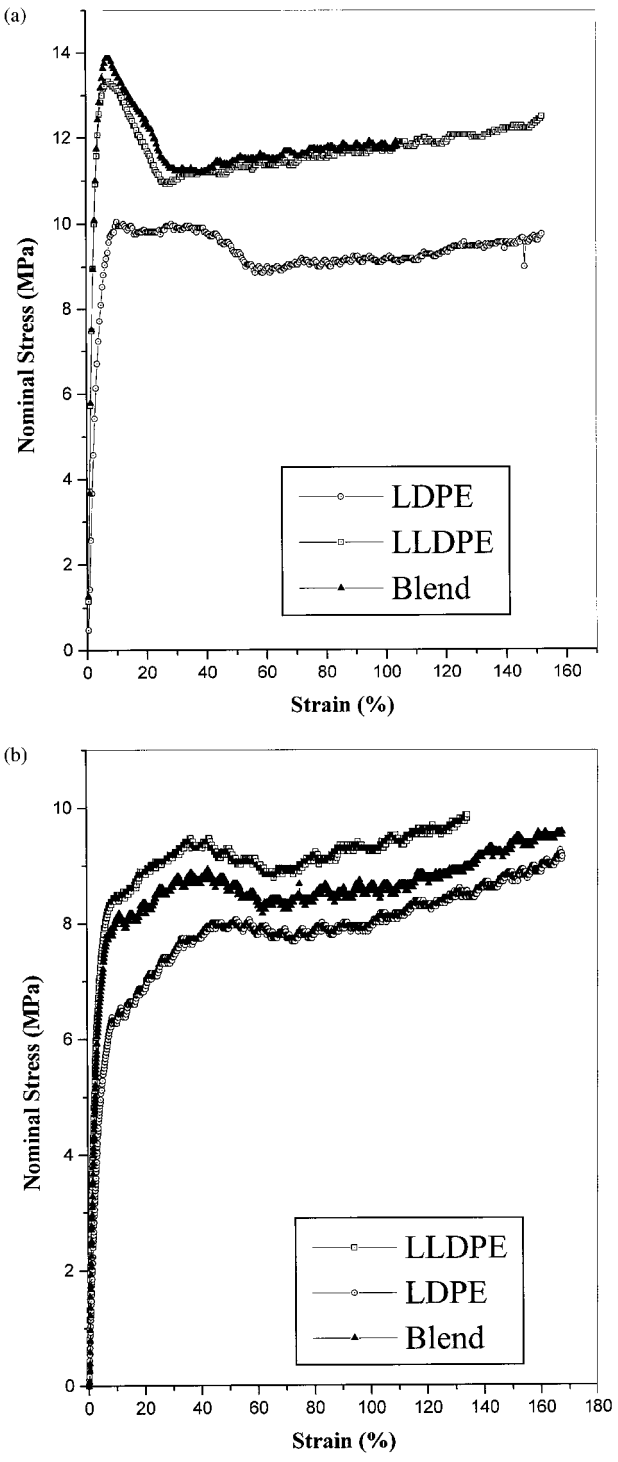

Figure 4 (a) Nominal stress–strain data for annealed materials; (b) nominal stress–strain data for quenched materials.

higher modulus and yield stresses for the LLDPE (*A*) and blend (*A*) samples, as can be seen in the DMA and tensile measurements (Figs. 3–5). As crystallinity does not change significantly with the thermal treatments, the differences in intercrystalline structural continuity must be responsible for the differences found in the modulus: The annealed samples show values which are about twice those measured for the quenched ones.

Nominal Stress-Elongation Curves

The deformation behavior and ultimate mechanical properties are very important characteristics of semicrystalline polymers. These macroscopic properties are known to depend very closely on the molecular structure and the level of crystallinity[6] so that their knowledge is considered essential.

LDPE displays lower yield stresses and an ultimate draw ratio than those of LLDPE at room temperature, as expected (Table III). Popli and Mandelkern[6] stated that branched specimens clearly display lower yield stresses than those of linear polymers of the same density. Besides the expected differences found between branched and linear polymers, large variations in behavior were induced by thermal treatments. For the samples used in this study, the already-mentioned differences are much more pronounced, due to the structural inhomogeneity of the LLDPE and the blend; also, thermal treatments induce larger effects, due to the segregation of the species with widely different melting points already mentioned.

Figure 4(a,b) displays nominal stress-elongation plots which were chosen to illustrate the two typical tensile behaviors observed. A cursory examination of the plots shows that the force-elongation curves follow one of two basic patterns: The annealed LLDPE (*A*) and blend (*A*) samples show a very sharp force maximum at low strain, corresponding to a yield point. Beyond this point, there is a decrease in the load with a further increase in elongation; the force then remains essentially constant with a further increase in length. In all quenched samples, and also in LDPE (*A*) [Fig. 4(a,b)], the maximum in load becomes much less defined, and a broader and slightly higher second load maximum appears.

Even if we did not find a significant change in crystallinity caused by the thermal treatments (Table I), but simply a change in the form of the DSC peak, significant changes in σy (Table III), in the force-elongation patterns, and in the DMA patterns were found. The highest σy values were displayed by the annealed samples of each mate-

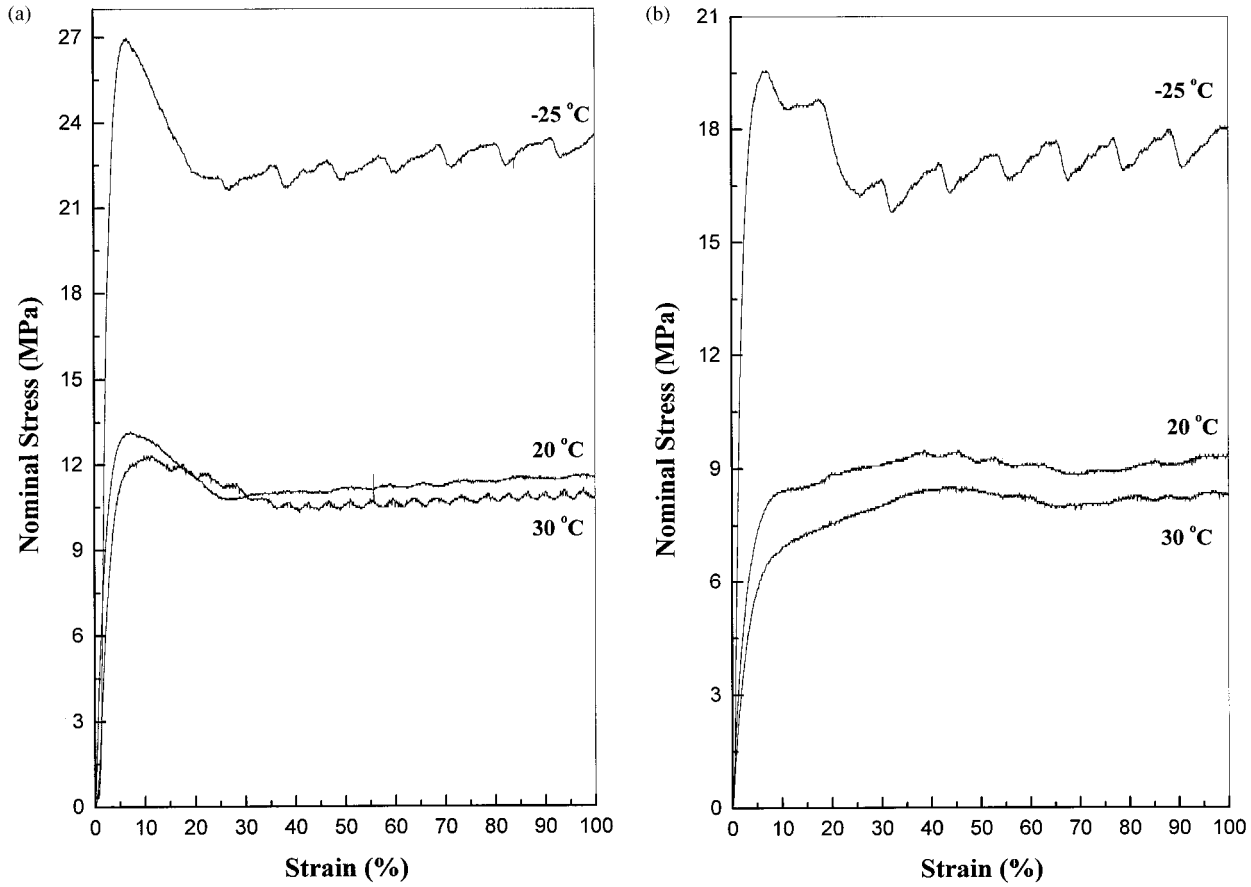

Figure 5 (a) Nominal stress–strain data for LLDPE (*A*) at different testing temperatures; (b) nominal stress–strain data for LLDPE (*Q*) at different testing temperatures.

rial type, even at the same crystallinity levels, due to the segregated—more continuous—semicrystalline structure with higher crystallinity and a higher melting point produced by the segregation effect of the annealing and slow cooling treatment. Drawability (λ_B in Table III) was practically not affected by the thermal treatments. This is expected, as this is a slow decrystallization–recrystallization process conducted at temperatures well above the glass transition.[23]

Table III Draw Ratios at Break and Yield Stress Values

Sample	Thermal Treatment	Testing Temperature (°C)	λ_B	σ_y (MPa)
LLDPE	Annealing	−25	>5.3	27.1
		20	6.7	13.1
		30	6.4	12.3
	Quenching	−25	>5.3	19.6
		20	6.6	9.5
		30	>7.5	8.5
LDPE	Annealing	20	4.8	9.6
	Quenching	20	4.9	8.0
Blend	Annealing	20	7.1	13.8
	Quenching	20	7.5	8.9

Samples subjected to the additional 2-h annealing at low temperature (−25°C) before mechanical testing at −25°C, also displayed increases in the σy and modulus, as measured by DMA and tensile testing, consistent with a very slight increase in crystallinity and the suppression of the β-relaxation process caused by the low testing temperature.

Variations in behavior induced by the testing temperature on the LLDPE nominal stress-elongation patterns are illustrated in Figure 5(a,b) and Table III. σy values decrease as expected with increasing temperature, and the predominant first yield point found at the low testing temperature is transformed into a more diffuse one when

the test is conducted at higher temperatures. These differences are much more noticeable for the quenched samples. This ought to be expected on the basis of the above-mentioned differences in the structural continuity between the annealed and quenched samples: For the quenched samples, a larger fraction of structural continuity (mechanical interconnection) is given through interphase material, which relaxes at temperatures above −25°C.

The presence of a double-yield point at room temperature in PE systems similar to ours was previously reported,[24,25] and different interpretations were given. Seguela and Rietsh[24] proposed that the yielding of MDPE involves two thermally activated rate processes, operating cooperatively but having different activation parameters relative to both the temperature dependence and the strain-rate dependence: slip of the crystal blocks past each other in the mosaic crystalline structure and a homogeneous shear of the crystal blocks. Brooks et al.[25] stated that the first yield point was associated with an intrinsic softening process within, and it was demonstrated that it could be partially or totally recovered. The second yield point was associated with permanent deformation. More recently, Lucas et al.[26] explained the development of double yields in terms of partial melting–recrystallization. This explanation seems to agree with that proposed in ref. 23.

Fracture Experiments

Load-displacement traces in the DENT experiments are sketched in Figure 6(a–c). The samples used for the tests shown in Figure 6 had all the same thickness and ligament length. In every case, the maximum net section stress is always slightly superior to the uniaxial yield stress for all ligaments lengths; this implies that all the ligaments were grossly yielded. Again, two basically different patterns—in coincidence with the two tensile drawing yield behavior patterns—were displayed:

LLDPE (*A*) and the blend (*A*) samples' load-displacement traces showed a well-defined maximum load point followed by a steep drop in stress which is coincident with the complete necking of the ligament [Fig. 7(a), point no. 3]. Photograph numbers coincide with the related numbers on the traces. Afterward, slow crack growth continues by ductile tearing beyond the inflection point, under plane-stress conditions, as the load dropped toward zero with a lower slope.

Load-displacement traces displayed by all quenched samples and LDPE (*A*) have a much less defined maximum load point followed by a drop in stress up to the inflection point, which is coincident with the complete necking of the ligament, this time less defined. Beyond this latter point [no. 3 in Fig. 7(b)], propagation continues in the same way as for annealed samples.

Variations induced by different testing temperatures in load-displacement traces are illustrated by Figure 8(a,b). As the testing temperature increases, the maximum load and the inflection point loose definition, and the absolute value for the maximum decreases. When going from −25 to 20°C, the major cause for this difference is the β-relaxation process, which at −25°C increases the stress needed for deformation and reduces the drawability by retarding the recrystallization process. When going from 20 to 30°C, the cause for the smaller change is considered to be the further advance into the crystalline α-relaxation temperature range.

From the areas under the load-displacement diagrams, the specific work of fracture, w_f, was calculated and plotted against the ligament length, L, as shown in Figures 9(a,b) and 10(a,b) and Table IV. The experimental data lie on a straight line which was extrapolated to give the specific essential work of fracture, w_e. It must be pointed out that the method leads to much larger errors in the determination of w_e than in βwp, as pointed out in Table IV. These data indicate that higher w_e values are related to combined higher σ_Y and COD values (see Table IV). This fact may be simply interpreted in terms of J_C, since w_e is equivalent to J_C[27] and J_C = COD σ_Y. σ_Y may be related to yield phenomena in the process zone, and COD, to the deformation process taking place in the highly stressed failure zone at the crack tip.

From the examination of Table IV, it appears that both the specific essential work of fracture and the specific nonessential work of fracture at room temperature have really poorer values for the LDPE samples than for the LLDPE samples, while the blend displayed practically the same behavior of the LLDPE within the experimental scatter. These results also agree with Hashemi and Williams[8] findings, who stated that when cracking does occur LDPE shows relatively low toughness values in spite of its drawability, and this seems to be simply a consequence of its low σ_Y.

No definite trend was found for w_e for radically different thermal treatments and testing temperature. Calculated w_e values superimpose in the

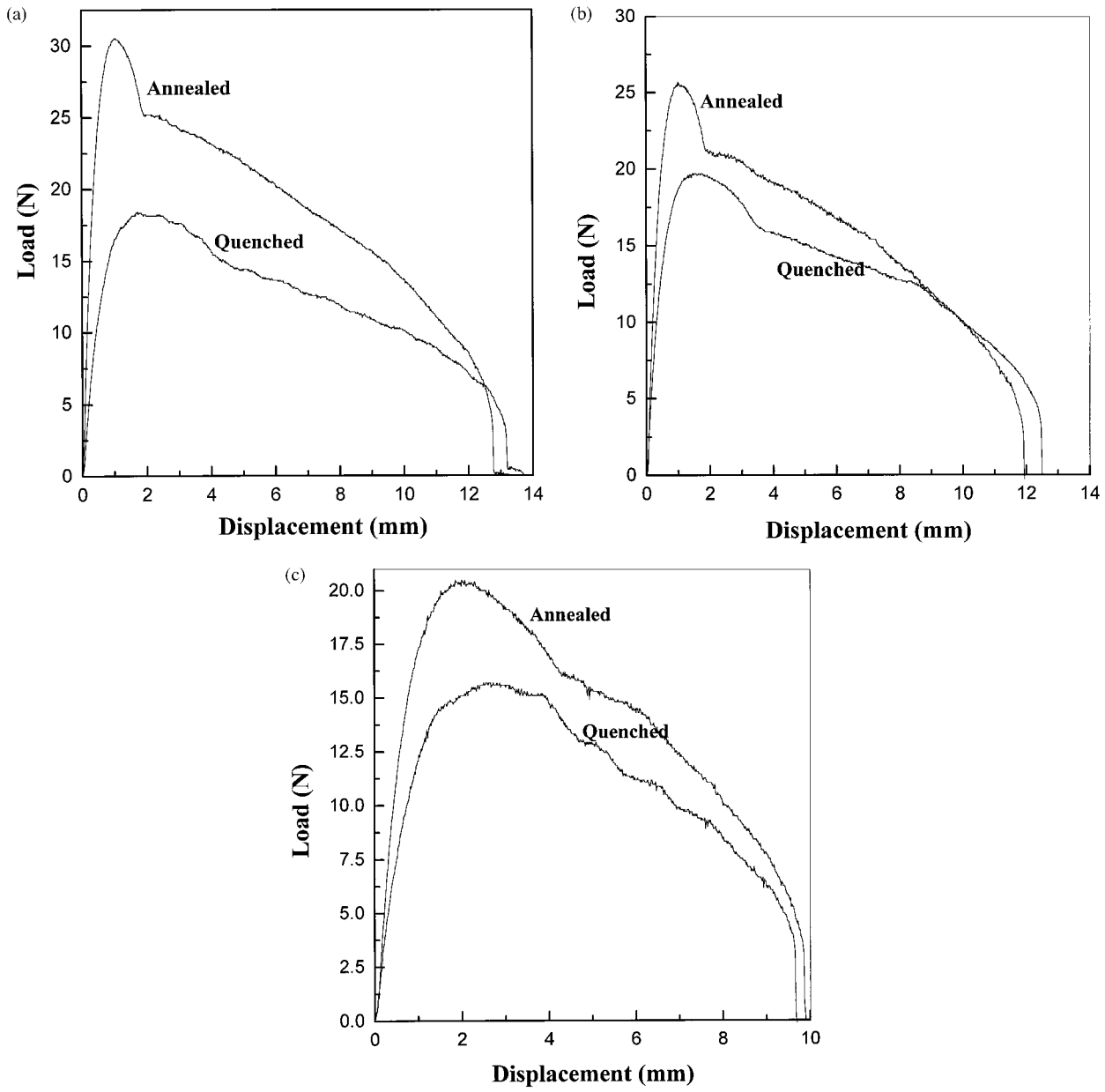

Figure 6 (a) Load-displacement traces of DENT specimens of similar dimensions, cut from LLDPE samples and tested at room temperature; (b) load-displacement traces of DENT specimens of similar dimensions, cut from BLEND samples and tested at room temperature; (c) load-displacement traces of DENT specimens of similar dimensions, cut from LDPE samples and tested at room temperature.

same statistical dispersion band (Table IV). The only exception was the significantly higher w_e values displayed by LLDPE at −25°C. This result seems to be consistent with the high σ_Y measured for these samples. However, the measured nonessential work of fracture, βw_p, (Table IV), which is a measure of the energy used for plastic deformation around the crack tip,[15] was always greater—within the experimental error—for annealed samples than for quenched samples, and it also displayed a decreasing trend with the increasing temperature.

From a phenomenological point of view, it can be argued that βw_p increases because annealed materials are capable of supporting much higher levels of load during the whole

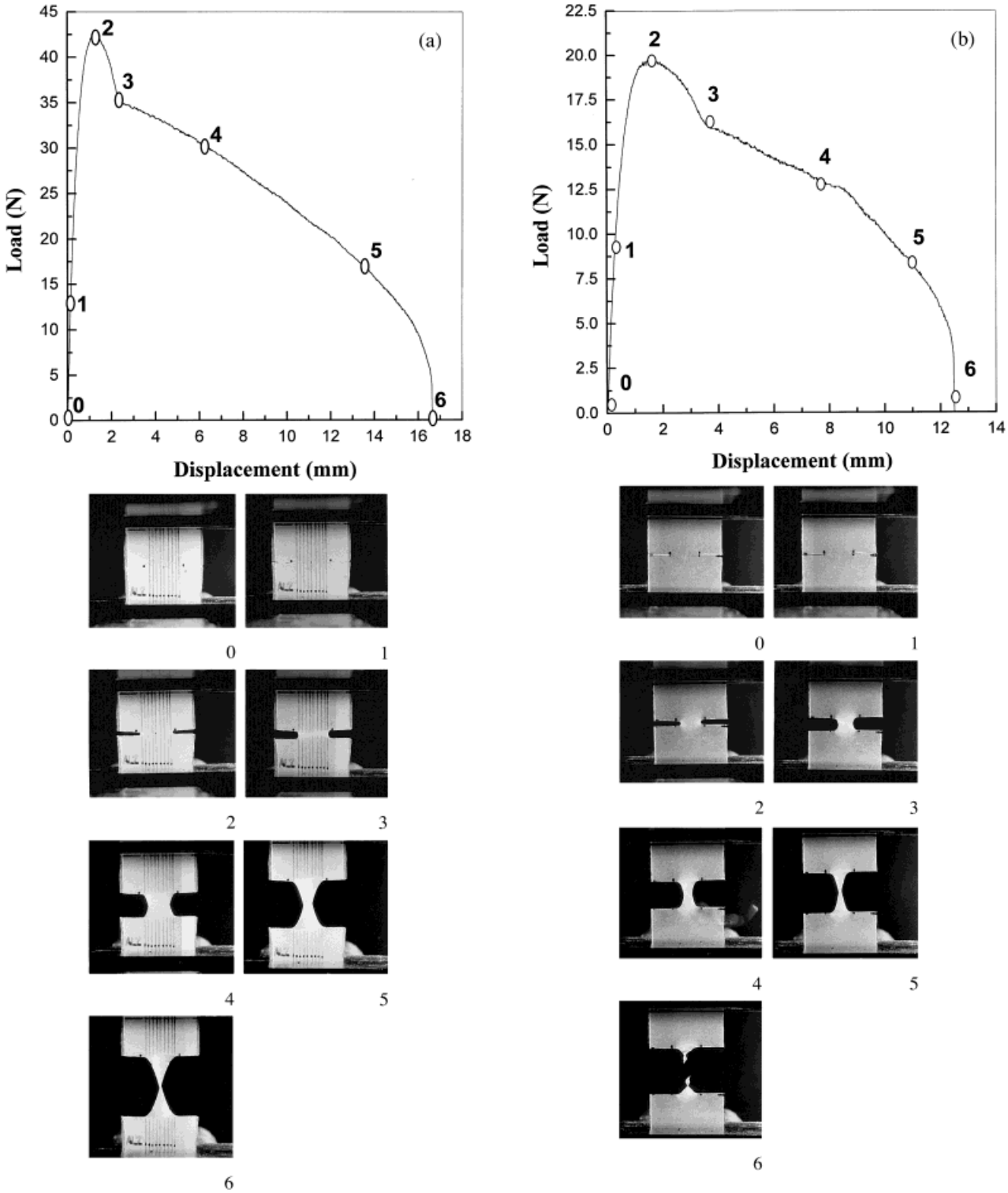

Figure 7 Load-displacement traces for (a) LLDPE (A) and (b) LLDPE (Q) and photograph sequences for points 0, 1, 2, 3, 4, 5, and 6 on the curves.

crack propagation with practically the same level of ultimate displacement. From a structural point of view, the more ordered (segregated) structure obtained by annealing supports higher levels of load than does the disordered, more homogeneous one obtained by

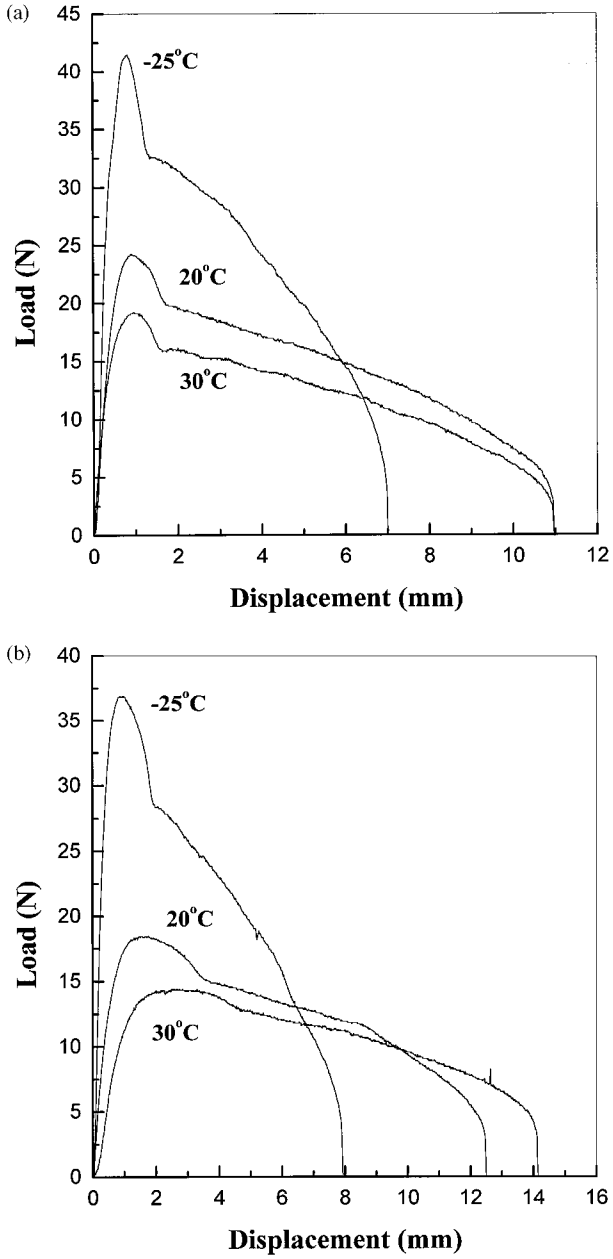

Figure 8 (a) Annealed materials: Load-displacement traces of specimens of similar dimensions, tested at different testing temperatures. (b) Quenched materials: Load-displacement traces of specimens of similar dimensions, tested at different testing temperatures.

quenching, mainly due to the differences in the intercrystalline structural continuity already mentioned. βw_p increases due to the higher stress needed for deformation, while drawability remains essentially the same.

The slow crack growth of PE at temperatures above the T_g has been visualized as a process of disentangling of the molecules within the amorphous region.[28] The tie molecules resisted the disentangling process by joining together the adjacent crystalline blocks. This simple picture disregarded the influence of the β-relaxation

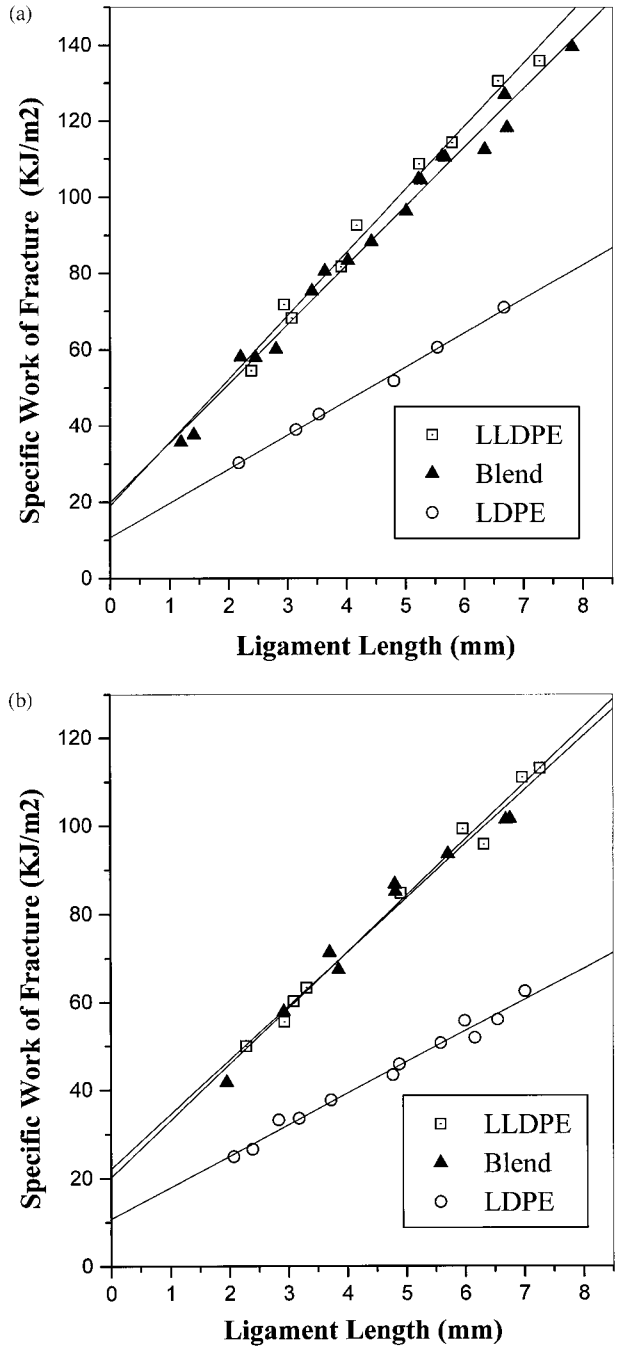

Figure 9 (a) Annealed materials: Specific work of fracture as a function of ligament length. (b) Quenched materials: Specific work of fracture as a function of ligament length.

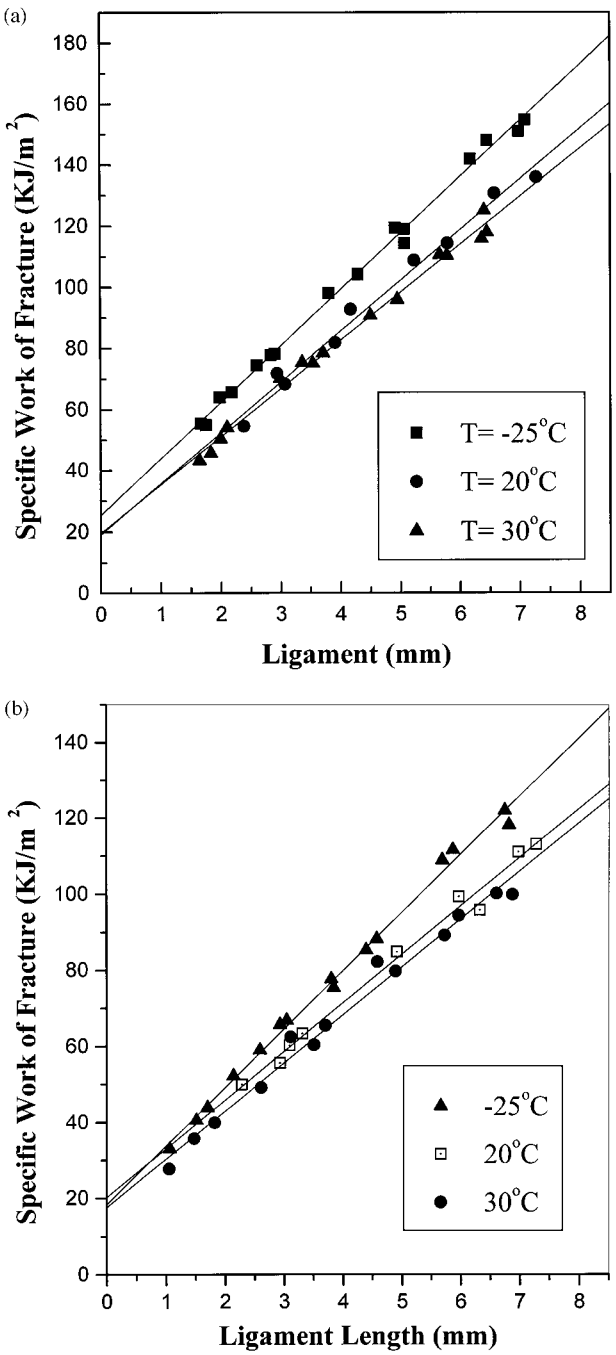

Figure 10 (a) Specific work of fracture for LLDPE (*A*) at different testing temperatures. (b) Specific work of fracture for LLDPE (*Q*) at different testing temperatures.

process, which is now shown to significantly influence the temperature dependence of these materials' slow fracture. Annealing promotes a much more continuous crystalline structure, which prevents the slipping of adjacent crystalline blocks and consumes more energy during crack propagation.

CONCLUSIONS

The essential fracture work concept has been successfully applied to characterize the fracture behavior of LDPEs under plane-stress conditions. All the samples, irrespectively of being pure materials or the blend, displayed geometrical similarity, as shown in Figures 8–10. This allows the essential work of fracture methodology to be applied.

Differences in the nominal stress-elongation curves and load-displacement traces (DENT precracked experiments) for the different polymers as well as between the same polymer following different processing procedures were found, which can be assigned to specific morphological differences. In standard tensile stress-elongation measurements, at room temperature, LDPE displays lower yield stresses and drawability than those of LLDPE and the blend, as expected. Consistently, the specific essential work of fracture and the specific nonessential work of fracture displayed poorer values fort LDPE samples than for the linear samples (LLDPE and blend).

The results reported here show that the tensile drawing and fracture behavior of the semicrystalline polymers studied is governed not only by the crystallinity but also by the changes in structural continuity. Drawability (λ_B) was practically not affected by the thermal treatments. The highest σ_y values were displayed by the annealed samples of each material type, even at almost the same crystallinity levels, due to segregation of polymer fractions which form semicrystalline structures with higher crystallinity and melting points which carry most of the tensile stress load.[18–21] Annealing promotes a segregated semicrystalline structure which prevents the slipping of adjacent crystalline blocks and consumes more energy during propagation in slow fracture experiments.

For molded (isotropic) samples, the overall fracture and mechanical behavior of the blend is practically the same as the one displayed by LLDPE, in spite of previous reports of Elmendorf[9] tests where blown films made from the blend gave better results. This is most probably due to fundamental differences between the Elmendorf test and the essential work of fracture method: The Elmendorf test does not require a fully yielded ligament prior to tear initiation at the notch tip

Table IV Fracture Parameters

Sample	Thermal Treatment	Testing Temperature (°C)	w_e (kJ/m^2)	Standard Deviation (w_e) (kJ/m^2)	βw_p (kJ/m^3)	Standard Deviation (βw_p) (kJ/m^3)	COD (mm)
LLDPE	Annealing	−25	25.4	1.5	18.5	0.3	1.3
		20	19.1	3.6	16.6	0.7	1.8
		30	19.6	1.7	15.7	0.4	1.6
	Quenching	−25	18.5	1.3	15.4	0.3	1.0
		20	22.2	2.4	12.8	0.5	2.4
		30	17.7	2.1	12.6	0.5	1.7
LDPE	Annealing	20	10.8	1.3	8.9	0.3	1.2
	Quenching	20	10.9	1.4	7.1	0.3	1.6
Blend	Annealing	20	20.0	2.2	15.5	0.5	1.3
	Quenching	20	22.3	4.0	12.3	0.8	2.0

and does not allow distinction between initiation and propagation stages. Furthermore, the propagation speeds used for both methods are widely different.

There is competition between the σ_Y and COD values, which determines the w_e values. Annealed samples exhibit a maximum in w_e at −25°C, coincident with the maximum in σ_Y, while quenched samples exhibit a maximum in w_e at 20°C, coincident with the maximum in COD.

The β-relaxation process strongly influences the fracture behavior at low-temperature testing, as shown in Figure 8: Samples fractured at −25°C displayed much higher load and less deformation, as expected when the relaxation of the crystalline-amorphous interphase is suppressed, increasing the tensile stress necessary for the semicrystalline structure deformation and restricting the recrystallization process present in the same samples fractured at room temperature. It is expected that medium or high-density PE, which has a smaller fraction of the amorphous-crystal interphase material, will be less influenced by the testing temperatures in this range.

Propagation consumes much more energy from the structure in LLDPE than in LDPE and from annealed samples than from quenched samples, as shown in Table IV (column for βw_p values). It looks like the nonessential work of fracture dissipated per unit volume of the material (w_p) is a much more sensitive parameter for these types of semicrystalline polymers which display similar displacements in the slow fracture of DENT specimens, with different load-bearing characteristics.

NOMENCLATURE

W_f	total work of fracture
W_p	nonessential work of fracture
W_e	essential work of fracture
L	ligament length
w_e	specific essential work of fracture
w_p	specific nonessential work of fracture
σ_y	yield stress
λ_B	draw ratio
r_p	plastic radius
COD	crack-opening displacement
δ	ultimate elongation
β	plastic zone shape factor
J_C	critical fracture initiation parameter
X_c	crystallinity index
T_{peak} (°C)	melting peak temperature.

REFERENCES

1. Rice, J. R. J Appl Mech ASME 35, 1968, 379.
2. Zhang, X. C.; Partridge, Y. K. In 9th International Conference on Deformation, Yield and Fracture of Polymers, Churchill College, Cambridge, UK, 1994; p 75.
3. Chan; Williams, J. G. Polymer 1994, 35, 1666.
4. Paton, C. A.; Hashemi, S. J Mater Sci 1992, 27, 2279.
5. Mai, Y. W.; Cotterell, B. Int J Fract 1986, 32, 105.
6. Popli, R.; Mandelkern, L. J Polym Sci Part B Polym Phys 1987, 25, 441.
7. Tielking, J. T. Polym Test 1993, 12, 207.
8. Hashemi, S.; Williams, J. G. Polymer 1986, 27, 384.
9. Elmendorf tearing test 42, ASTM d-1922-67.
10. Broberg, K. B. Int J Fract 1968, 4, 11.

11. Wu, J.; Mai, Y. W. Polym Eng Sci 1996, 36, 2275.
12. Noticiero del Plástico (Buenos Aires) 366 (60).
13. Melkern, L.; Allow, A. L.; Fopolan, M. J Phys Chem 1965, 72, 309.
14. Wang, M. D.; Nakanishi, E.; Hashizume, Y.; Hibi, S. Polymer 1992, 33, 2715.
15. Mai, Y.-W.; Powell, P. J Polym Sci Part B Polym Phys 1991, 29, 785.
16. Hashemi, S. J Mater Sci 1993, 28, 6178.
17. Hashemi, S.; O'Brien, D. J Mater Sci 1993, 28, 3977.
18. Hill, H. J. Mech Phys Solids 1952, 4, 19.
19. Mirabella, F. R. Paper presented at Advances in Polyolefins Workshop, ACS, Napa, CA, 1997.
20. Balsara, N. P.; Fetters, L. J.; Hadjichristidis, N.; Lohse, D. J.; Han, C. C.; Graessley, W. W.; Krishnamoorti, R. Macromolecules 1992, 25, 6137.
21. Crist, B.; Nesarikar, A. R. Macromolecules 28, 890, 1995.
22. Failla, M. D.; Carella, J. M. J Polym Sci Part B Polym Phys 1988, 26, 2433.
23. Brady, J. M.; Thomas, E. J. J Mater Sci 1989, 24, 39.
24. Seguela, R.; Rietsh, F. J Mater Sci Lett 1990, 9, 46.
25. Brooks, N. W.; Duckett, R. A.; Wards Rietsh, I. M. Polymer 1992, 33, 1872.
26. Lucas, J. C.; Failla, M. D.; Smith, F. L.; Mandelkern, L. Polym Eng Sci 1995, 35, 117.
27. Wu, J.; Mai, Y.; Cotterell, B. J Mater Sci 1993, 28, 3373.
28. Huang, Y.-L.; Brown, N. J Polym Sci Part B Polym Phys 1991, 29, 129.